A critical view of computational chemistry methods in understanding corrosion inhibition of 6-chloro-2-phenylimidazo[1,2-*b*]pyridazine in 1 M and 5 M HCl

N. Achnine,[1] M. Driouch,[1]* A. Elhaloui,[1] Z. Lakbaibi,[2,3] El H. El Assiri,[1] M. Kadiri,[1] M. Sfaira,[1] O. Dagdag,[4] A. Berisha,[5] B. El Ibrahimi,[6] S. Kaya,[7] L. Guo[8] and A. Zarrouk[9]**

[1]Laboratory of Engineering, Modelling and Systems Analysis (LIMAS), Faculty of Sciences, Sidi Mohamed Ben Abdellah University, 30000, Fez, Morocco
[2]Molecular Chemistry, Materials and Environment (LCM2E), Multidisciplinary Faculty Nador, University Mohammed the First, Mohammed V avenue, P.O.Box 524, Oujda 60000, Morocco
[3]Laboratory of Analytic and Molecular Chemistry (LCAM , Faculty Polydisciplinary of Safi, Cadi Ayyad University, 46030 Safi, Morocco
[4]Centre for Materials Science, College of Science, Engineering and Technology, University of South Africa, Johannesburg 1710, South Africa
[5]Department of Chemistry, Faculty of Natural and Mathematics Science, University of Prishtina, 10000 Prishtina, Kosovo
[6]Department of Applied Chemistry, Faculty of Applied Sciences, Ibn Zohr University, 86153, Aït Melloul, Morocco
[7]Department of Chemistry, Faculty of Science, Cumhuriyet University, Sivas 58140, Turkey
[8]School of Material and Chemical Engineering, Tongren University, Tongren, 554300, China
[9]Laboratory of Materials, Nanotechnology and Environment, Faculty of Sciences, Mohammed V University, Av. Ibn Battuta. P.O. Box 1014, Rabat, Morocco
**E-mail: majid.driouch.fsdm@gmail.com; azarrouk@gmail.com*

Abstract

The aim of this article is to highlight some of the pitfalls frequently encountered in the literature. Firstly, deductions based on correlations obtained for a few isolated inhibitors. Secondly, the inability of quantum methods to account for the aggressiveness of the environment. Thirdly, distrust in the interpretation of small differences between energy descriptors in terms of correlation between experimental results and quantum calculations. Finally, the use of overly simplistic surface models. This study highlights the limitations of local reactivity descriptors such as EPF and NPF calculated according to NBO and not according to NPA for the isolated molecule 6-chloro-2-phenylimidazo[1,2-*b*]pyridazine in both its neutral CP-IPZ and protonated CP-IPZH forms. Also, the calculation of NEBD according to QTAIM, then the calculation of GEDT at the level of the transition states of the iron-CP-IPZH complex. The resulting

descriptors take no account of the nature or concentration of the corrosive medium (1 M and 5 M HCl). In addition, DM and MC were used to take account of the concentration of the corrosive solution, inhibitor-metal interactions and the dynamic aspect of the adsorption process. It was shown that despite the difference in adsorption energy of CP-IPZH, which follows the trend in terms of the aggressiveness of the medium, does not reflect the low polarization resistance in 5 M HCl, *i.e.* ten times lower than that in 1 M HCl.

Keywords: *acid corrosion, 1 M and 5 M HCl, DFT, NBO, QTAIM, NBED, GEDT, MD and MC simulations.*

Received: June 17, 2023. Published: July 10, 2023 doi: 10.17675/2305-6894-2023-12-3-6

1. Introduction

Over the last decade, many researchers have made frequent use of quantum chemistry and/or molecular dynamics approaches to understand the corrosion inhibition mechanism of organic compounds. The aim of these calculations is to gain a better understanding of the details at the atomic scale, to interpret experimental results and to predict new corrosion inhibitors [1–10]. The above approaches often require approximations to make the calculations feasible. These approximations can introduce systematic errors that limit the accuracy of the results obtained [1, 2, 4].

The conventional MEPTIC (molecular electronic properties to inhibition-efficiency correlation) approach, which is still relevant today, involves determining the structural, electronic and energetic parameters of inhibitor molecules in the isolated state, in both the gas and aqueous phases, by implicitly treating the solvent using polarizable continuum models in order to correlate them with the inhibitor efficiencies obtained experimentally using electrochemical methods. Indeed, the structural and electronic properties of inhibitors, generally derived from density functional theory (DFT), are used to conjecture trends in the adsorption bonds of various inhibitor molecules with the metal matrix surface [1–6].

Among the descriptors calculated, according to the literature using DFT theory, are the energies of the molecular frontier orbitals; the highest occupied (HOMO) and the lowest vacant (LUMO), from which the HOMO–LUMO energy gap is deduced, parameters that play a crucial role in the theory of hard and soft acids and bases (HSAB) such as electronegativity, chemical hardness or softness, and the rate of electron transfer from the inhibiting molecule to the surface [1, 7]. In addition to these global parameters, other local properties such as reactivity indices based on Fukui functions, atomic charges, molecular electrostatic potential maps and the spatial distribution of HOMO and LUMO orbitals are also considered relevant [1, 3].

However, it is important to remember that no attention is paid to the substrate and the stability of the inhibitors in the corrosive solution, *i.e.* possible acid-base, complexation or precipitation reactions, or even redox reactions during polarization of the electrochemical interface. As a result, the MEPTIC approach has widely been debated and criticized both conceptually and statistically in the literature by Kokalj *et al.* [1, 3–5]. For example, Kokalj

openly states that there is no direct link between structural and electronic properties and corrosion inhibiting efficacy, and that the relationship is much more complex. In addition, N. Kovacevic *et al.* [8] have pointed out that, in general, certain organic compounds may eventually undergo reactions with the constituents of the medium, leading to the formation of new products. In this case, the intrinsic electronic properties of the inhibitors initially introduced into the corrosive solution should not be correlated with inhibitory efficacy.

In addition, the correlation between the electronic properties of stable molecules, apart from the effect of solvation or interaction with the metal matrix, and their inhibiting power is a second warning. Whatever the level of theoretical calculation considered, however important it may be, the study of the inhibitor-surface bond remains insufficient to explain the effectiveness of a corrosion inhibitor. Consequently, other effects must also be taken into account.

Furthermore, Lindsay *et al.* [9] have argued that in terms of predictive character, such an approach can easily be misleading due to the complexity of the corrosion inhibition phenomenon where a variety of factors can influence inhibitory efficacy. These include the nature of the corrosive solution and its chemical characteristics, temperature, the chemical composition of the samples and their surface conditions. In practice, it is commonly accepted that the surface of steels is perfectly smooth, with a simple crystallographic orientation, but in reality, it is generally jagged and riddled with structural defects. These different factors do not intervene individually, but in a more or less complex relationship with each other. The confluence of these different factors makes it impossible to envisage a systematic correlation between experimental results and quantum computation. If one of the determining factors is not taken into account, the results may be misinterpreted and lead to erroneous conclusions.

To remedy this, it would be advisable, if possible, to model rigorously the interactions between the various components of the corrosion system. Recently, several efforts have been made to improve the reliability of theoretical calculations [1, 3]. Consequently, the theoretical study can only be useful and effective if there is sufficiently convincing and correct modeling of the reality of the interfacial processes. On the contrary, they aim to emphasize that when the factors are carefully modeled and the results intelligently interpreted, the understanding of the corrosion process and its inhibition can be greatly improved.

The aim of this work is to highlight a comparison between theoretical results and the corresponding experimental data in order to identify the pitfalls to be avoided if a theoretical calculation is not to be misinterpreted. To do this, we chose to study the corrosion of a C38 mild steel and its inhibition by an organic molecule derived from imidazo-pyridazine, 6-chloro-2-phenylimidazo[1,2-*b*]pyridazine (CP-IPZ), in two acidic media of very different aggressiveness. The polarization resistances obtained using electrochemical impedance spectroscopy, at the optimum concentration of $10^{-3}\,\mathrm{mol\cdot L^{-1}}$ of CP-IPZ, are 1016 and $94\ \Omega\cdot\mathrm{cm}^2$ respectively, with inhibitory efficiencies of 94 and 88% in 1 M HCl and 5 M HCl. These experimental results are the subject of an exhaustive electrochemical study, submitted for publication, comparing different electrochemical techniques (EVT, PEIS, CASP, VASP,

LPR and TAFEL Plot). In addition, the method used to synthesize and characterize the CP-IPZ inhibitor molecule using ^{1}H, ^{13}C and FTIR NMR was described, as was the time-dependent stability of this molecule in the corrosive solution using HPLC-MS.

In the present work, the theoretical study that we have carried out concerns the consideration and verification of the stability, as a function of pH, of the inhibitor molecule studied by means of a Marvinsketch study. In addition, three theoretical approaches (DFT), natural bond orbitals (NBO) theory and quantum theory atomic in molecules (QTAIM) were used to understand and predict the behavior of the CP-IPZ molecule, its reactivity and its chemical properties. Each of these approaches offers specific advantages and limitations, and their choice often depends on the nature of the problem being studied and the computational resources available.

In addition, numerical simulation approaches (molecular dynamics (MD) and Monte Carlo (MC)) are used to simulate the interactions between inhibitor molecules and the metal surface, as well as the corrosion processes that occur on an atomic scale, and to predict the adsorption properties of the inhibitor on the metal surface.

2. Calculation Details

2.1. Partial charge calculation using Marvinsketch software

The Charge plugin implemented in Marvinsketch software is used to calculate the value of the partial charge of each atom of the compound 6-chloro-2-phenylimidazo[1,2-*b*]pyridazine. The charge is expressed in atomic units.

2.2. Theoretical calculations procedure

The NBO (natural bond orbitals theory), DFT (density functional theory), and quantum theory atomic in molecules (QTAIM) are three consistent theoretical approaches that are used to give more supplementary information regarding the molecular structure of inhibitor (CP-IPZH) and understand its reactivity behaviour towards iron surface [11]. Optimization of the inhibitor's structure was carried out using the self-consistent field (SCF) calculations including Kohn-Sham (KS) theory (DFT) with hybrid functional B3LYP by 6-311G+(d, p) basis set for hydrogen, carbon, nitrogen chlorine atoms, and to the basis set LanL2DZ level for iron atoms at transition states (TSs) [11]. The active sites existing within the compound CP-IPZH have been analysed according to the local reactivity indices such as electrophilic Parr functions EPF (for electrophilic attack) and nucleophilic Parr function NPF (for nucleophilic attack) based on the Mulliken atomic spin density (MASD) calculations that achieved in terms of natural bond orbitals theory (NBO) and not in terms of natural population analysis (NPA) that we criticized in this work. The partial atomic charge and non-bonding electron density (NBED) for the main atoms of CP-IPZH were calculated at the level of the NBO and QTAIM theories, respectively. These calculations were done in the aqueous phase through an implicit solvation model (SMD) *via* Gaussian 09 Revision-D.0l [11, 12]. The TSs of the corresponding complexes "inhibitor Fe" were localized using

transition state theory on the basis of second-order Gonzalez-Schlegel integration quadratic synchronous transit-guided quasi-Newton (QST2) approach using B3LYP functional at DFT method. The global electronic density transfer (GEDT) at the TSs was calculated as the sum of the natural atomic charges, found through an NBO analysis, of the atoms belonging to both donor and acceptor fragments characterized the TSs structures [11]. The direction of the electron density flux takes place from the donor fragment (positive value of GEDT) to the acceptor fragment (negative value of GEDT).

2.3. MC and MD simulations procedure

The modeling of interfacial interactions between inhibitor molecule and metal surface was studied using Monte Carlo (MC) and molecular dynamic (MD) simulations in aqueous phase [13–15]. MC and MD calculations were carried out in a simulation box of 24.823752 Å×24.823752 Å×53.241658 Å dimensions, which composed from six Fe(110) layers and 35 Å as a vacuum region. To mimic solution phase [16], the following formulation, with one inhibitor molecule, were adopted with: $600H_2O+5H_3O^+ +5Cl^-$ (1 M HCl medium) and $600H_2O+25H_3O^+ +25Cl^-$ (5 M HCl medium) ions system on Fe(110) surface. In this work, MD simulations were performed with NVT canonical ensemble for a simulation time of 700 ps with 1.0 fs as a time step [17]. The temperature of the studied systems was fixed at 298 K by means of the Berendsen's thermostat. Herein, the COMPASS III (Version 1.0 was used as a force field to calculate the interaction energies between inhibitor molecules and metal surfaces, and to estimate the associated thermodynamic and kinetic properties. Atom-based and Ewald summation methods are used to accurately and realistically calculate Van der Waals and non-bonding electrostatic interactions, contributing to more accurate modeling of interactions between inhibitor molecules and metal surfaces, respectively [18]. To account the effect of solution on the protonation state of inhibitor molecule, both neutral and protonated forms were considered during MC and MD simulations. The adsorption energy (E_{ads}) was estimated using Equation (1) [19, 20].

$$E_{ads}=E_{(110)/inhibitor}-E_{Fe(110)}-E_{inhibitor} \quad (1)$$

where $E_{(110)//inhibitor}$, $E_{Fe(110)}$ and $E_{inhibitor}$ are the potential energies of the inhibitor/surface system, the bare surface and the isolated inhibitor respectively.

Generally, the type of interfacial interactions between adsorbate and adsorbent can be predicted based on the length of potential established bond. For this, the pair correlation function, currently known as the radial distribution function ($g(r)$), was analyzed. This function (2) is defined as the probability of finding the particle B within the range ($r+dr$) around the particle A [21].

$$g_{AB}(r)=\frac{1}{(\rho_B)_{local}}\cdot\frac{1}{N_A}\sum_{i\varepsilon A}^{N_A}\sum_{i\varepsilon B}^{N_B}\frac{\delta(r_{ij}-r)}{4\pi r^2} \quad (2)$$

3. Results and Discussion

3.1. In silico approach studies

The chemical properties of inhibitors, as well as their protective power, depend largely on their ability to be ionized in aqueous solution. Most molecules contain specific functional groups that can accept or release protons in particular circumstances. Each ionization equilibrium between the protonated and deprotonated forms of the molecule can be described by a constant value called pK_a [6]. The ratio between protonated and neutral forms is closely dependent on pH, temperature and the ionic activity of the bulk phase. The ionization constant K_a, at a temperature T, is obtained from the activity ratio of the base and its conjugate acid, multiplied by the proton activity. The distribution of partial charges is a key factor in determining many of a molecule's physicochemical properties, such as ionization constants, reactivity, *etc.*

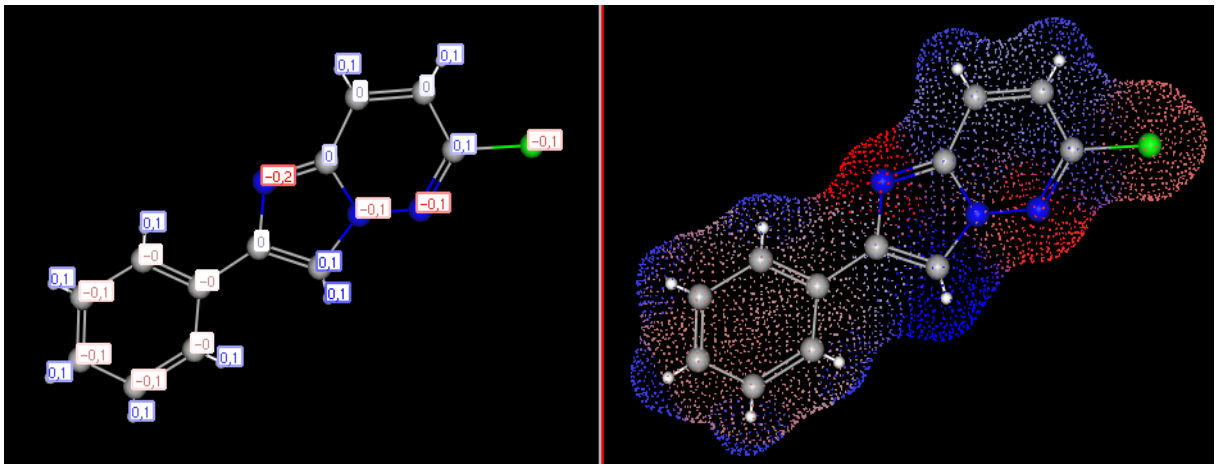

Figure 1. Partial charge values of each atom of CP-IPZ inhibitor.

Analysis of Figure 1 shows that the unsaturated N atoms (–N=C) of imidazole and pyridazine have a rich electron density (in red). These two sites appear to have a tendency to be protonated in an acidic environment. In fact, their free electron pair is not involved in aromaticity, since the p orbital is already engaged to form a π bond (its pair is therefore in a sp^2 hybridized molecular orbital). On the other hand, the nitrogen atom common to the imidazole and pyridazine nuclei is not likely to be protonated, despite having a density of –0.1*e*; in fact, it hybridizes in sp^2 and places its doublet in a pure *p* orbital in order to participate in conjugation.

Like the partial charge, the distribution is highly sensitive to the protonation-deprotonation process (near and far from the protonation site). The pK_a values of all atoms that gain or lose protons are calculated at 298 K, using Marvin software, on the basis of the partial charge distribution. Figure 2 shows the distribution of microspecifics/macrospecifics as a function of pH.

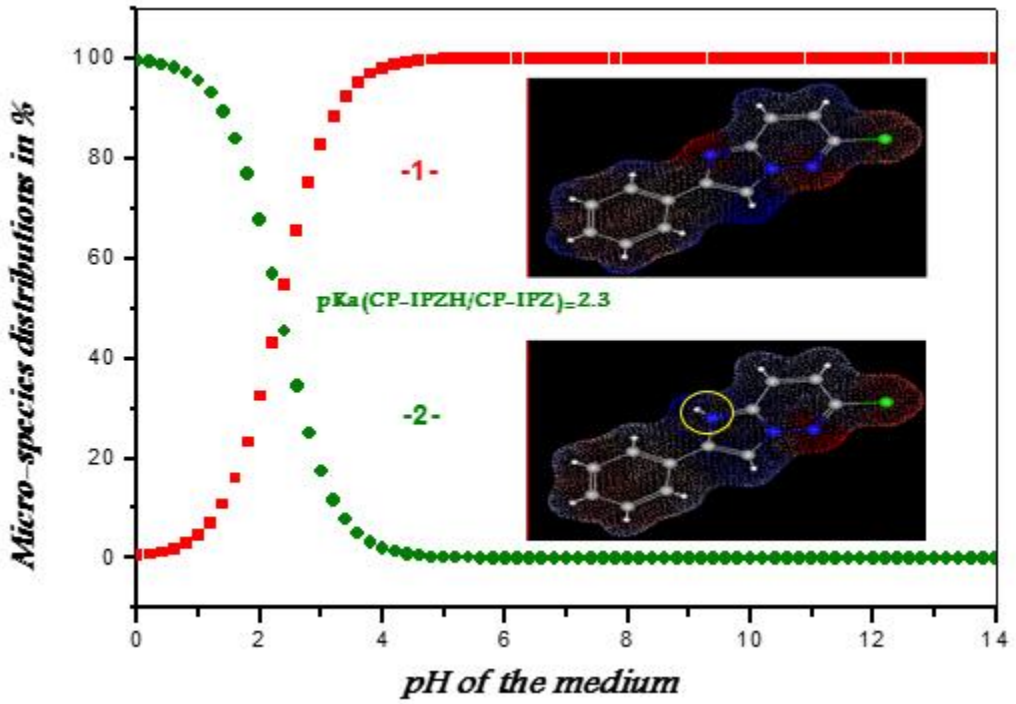

Figure 2. Distribution diagram of CP-IPZ micro-species at T=298 K and at different pH of the medium.

On Figure 2, it can be seen that 6-chloro-2-phenylimidazo[1,2-*b*]pyridazine {CP-IPZ} is a base capable of protonating in an aqueous solution on the unsaturated nitrogen atom (–N=C) of imidazole to give rise to the formation of its conjugate acid 6-chloro-2-phenylimidazo[1,2-*b*]pyridazin-1-ium {CP-IPZH}. This pair (CP-IPZH/CP-IPZ) is characterized by pK_a=2.3.

In the corrosive solution of molar or five times molar hydrochloric acid, the pH of the solution remains below the pK_a–2 value, so that the compound CP-IPZ (neutral form) has a percentage distribution approaching 0%. This suggests that the CP-IPZ form is highly unstable and transforms entirely into CP-IPZH (protonated form), becoming an ultra-majority form with a percentage of almost 100%.

Figure 3 represents the structure of the majority form of protonation at pH=0.

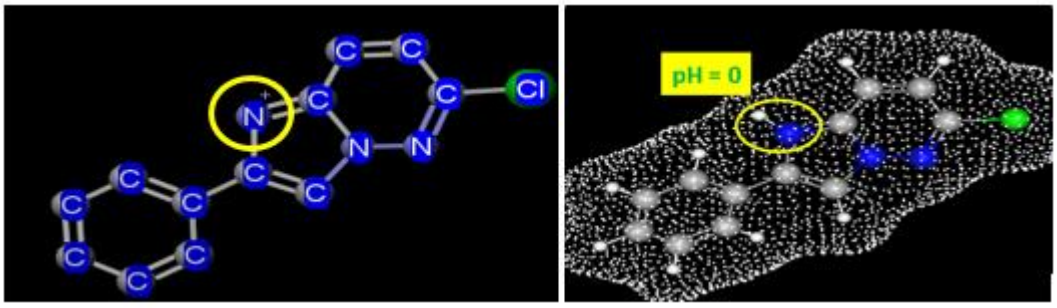

Figure 3. Structure of the majority protonated form of CP-IPZ inhibitor at pH=0.

The partial charge value of each atom of the compound 6-chloro-2-phenylimidazo[1,2-*b*]pyridazin-1-ium is given in Figure 4.

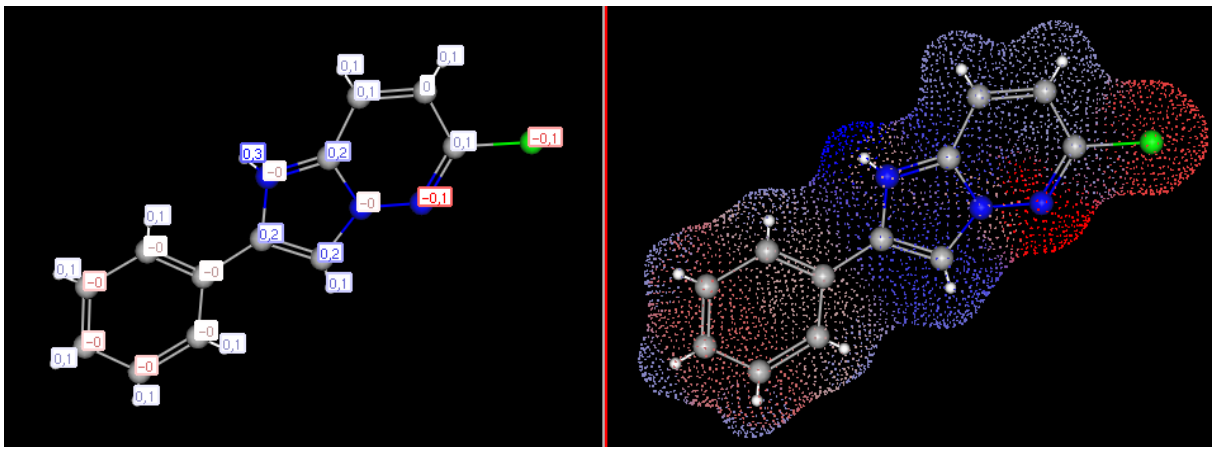

Figure 4. Partial charge value of each atom of CP-IPZH.

Analysis of Figure 4 shows that the partial charge distribution of the protonated nitrogen (–N+=C) on the imidazole ring and its neighboring atoms in the CP-IPZH structure (acid form) is very different from that observed in the CP-IPZ structure (base form). This shows that this distribution is highly sensitive to the protonation-deprotonation process. Secondly, since corrosion inhibition is mainly controlled by physical or chemical adsorption of the inhibitor onto the steel surface, it would be imperative to take protonation into account for a better understanding of the inhibition mechanism.

Using Marvinsketch software, based essentially on highlighting the partial charges on the various atoms of the CP-IPZ inhibitor molecule, it was found that, irrespective of the nature of the corrosive medium (1 M or 5 M HCl), and the majority form acting as inhibitor is only the protonated form. On the other hand, the experimental study revealed that the 5 M HCl solution was 10 times more aggressive than the 1 M HCl solution, with polarization resistances increasing from 94 to 1016 $\Omega \cdot cm^2$. This comparison of experimental results and theoretical calculation shows that the calculation cannot predict the adsorption capacity of this inhibitor molecule, given the corrosivity of both media.

Thus, identifying the structure of the majority compound in the corrosive solution and calculating the distribution of partial charges on its various atoms are by no means the exclusive factors determining inhibition efficiency (%*IE*). In fact, corrosion inhibition is a much more complex phenomenon, depending on the interaction of a variety of contributing factors (*cf.* Introduction).

3.2. Theoretical results

Concerning the quantum descriptors adopted for the prediction of the overall reactivity of the inhibitor towards the metal surface in the literature, we have frequently cited them as follows the energy gap HOMO/LUMO, the gap back/donating, global chemical hardness, global chemical softness, electron affinity, electronegativity, global electrophilicity, global

nucleophilicity and so on [1, 22–24]. However, when we return to the relationship dedicated to the calculation of these descriptors, we mentioned that they are directly linked to the HOMO's and LUMO's energies that characterize the molecular structure of the inhibitor. Here, we would like to ask the following questions:

1. Is the reactivity (whether global or local) of a molecule always governed by the electron density located at the molecular frontier orbitals (HOMO and LUMO)!!?
2. If this reasoning is correct, what will be the position of the quantum model that its principle is based on the probabilistic existence of the electron (electron density) and not according to the classical model that considers localization of electrons (*e.g.* Lewis model for bond construction)!!?

According to the literature [1, 3], the active sites existing in an organic molecule of the inhibitor are more often determined based on the Fukui indices such as Fukui functions f^- (electrophilic attack) and f^+ (nucleophilic attack) which are calculated in terms of the natural population analysis (NPA) theory. However, from the literature, the NPA analysis requests just the natural population calculations in which atomic partial charges (natural charges) are obtained through summation over natural atomic orbitals. In the contrary, the NBO analysis requests a full natural bond orbital analysis in which atomic charge is evaluated through electron density that is delocalized within all molecular systems. This indicates that the NBO calculations will be more consistent than the NPA ones to evaluate perfectly the local reactivity behaviour of the studied structure of CP-IPZH.

3.2.1. Local reactivity behavior of CP-IPZH

To determine the active centers of the inhibitor molecule, EPF and NPF functions, charge distribution (CD) and non-bonding electron density (NBED) were considered and discussed. So, regarding the adsorption process, atomic sites on a molecule with a high value of EPF or enough value of NBED behave like nucleophilic atomic sites when they react with iron atoms' surface to form covalent bonds. Also, atomic sites with a high value of NPF or not enough value of NBED may be responsible for forming coordination bonds by accepting electron density from the metal. Generally, the atomic centers with a negative or negligible value of Parr indices are considered as not active centers. QTAIM analysis is widely exploited to make clear the bonding and non-bonding regions in a molecular system, by calculating the electron density that circulates within the molecular system. This calculation allows also an evaluation of the probability of finding an electron in the area space of a reference electron located at a given point and with the same spin. Physically, this event the amount of spatial localization of the reference electron and offers a method for the plotting of electron pair probability in a molecular system. There are two types of electron density that circulate within a molecular system such as bonding electron density (BED) and non-bonding electron density (NBED).

3.2.1.1. NBO charge distribution and Parr functions analysis

The results of the charge distribution (CD) obtained according to natural bond orbitals analysis (NBOA) calculations are analyzed and discussed for the most active sites of CP-IPZH. A schematic illustration of the CD is given in Table 1 and Figure 5. EPF and NPF values of CP-IPZ and NPF and CD values of CP-IPZH are calculated for the main atoms of the CP-IPZH (Table 1 and Figure 5).

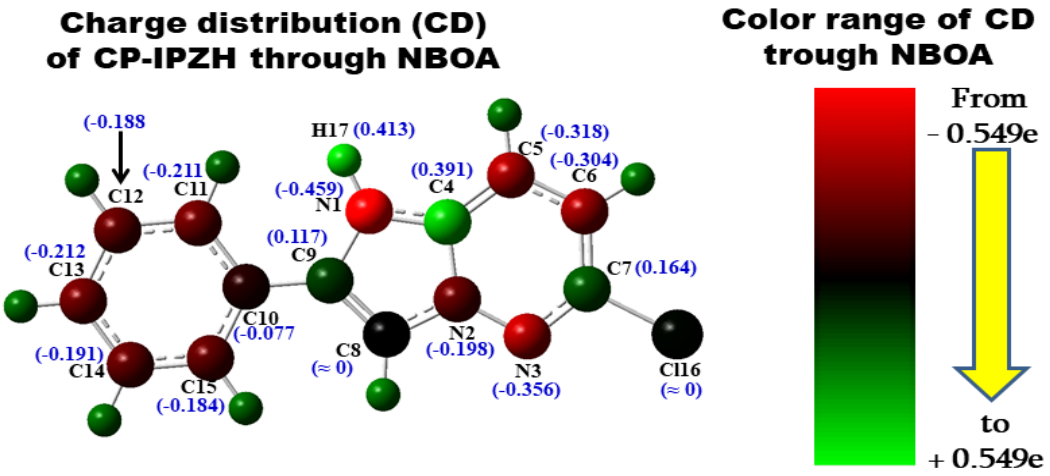

Figure 5. Charge distribution values (in parenthesis) around atomic sides of CP-IPZH inhibitor obtained according natural bond orbitals analysis (NBOA).

Table 1. Calculated Parr functions EPF and NPF (for CP-IPZ) and NPF (for CP-IPZH).

Atom	No.	EPF (CP-IPZ)	NPF (CP-IPZ)	NPF (CP-IPZH)	CD (CP-IPZH)
N	1	0.312	–0.055	0.060	–0.456
N	2	0.008	–0.028	0.093	–0.198
N	3	0.074	0.006	0.448	–0.356
C	4	–0.068	0.139	–0.012	0.391
C	5	0.400	–0.072	0.183	–0.318
C	6	0.112	0.141	0.257	–0.304
C	7	0.037	0.012	–0.092	0.164
C	8	–0.056	0.3488	–0.098	≈0
C	9	–0.056	0.1028	0.141	0.117
C	10	–0.005	0.158	–0.036	–0.077
C	11	0.073	0.073	0.052	–0.211
C	12	–0.018	–0.053	0.021	–0.188
C	13	0.094	0.252	0.052	–0.212

Atom	No.	EPF (CP-IPZ)	NPF (CP-IPZ)	NPF (CP-IPZH)	CD (CP-IPZH)
C	14	–0.009	–0.069	–0.019	–0.191
C	15	0.037	0.075	0.033	–0.184
Cl	16	–0.002	0.021	–0.007	≈0

Note to Table 1: negative null values of EPF and NPF are considered not reactive.

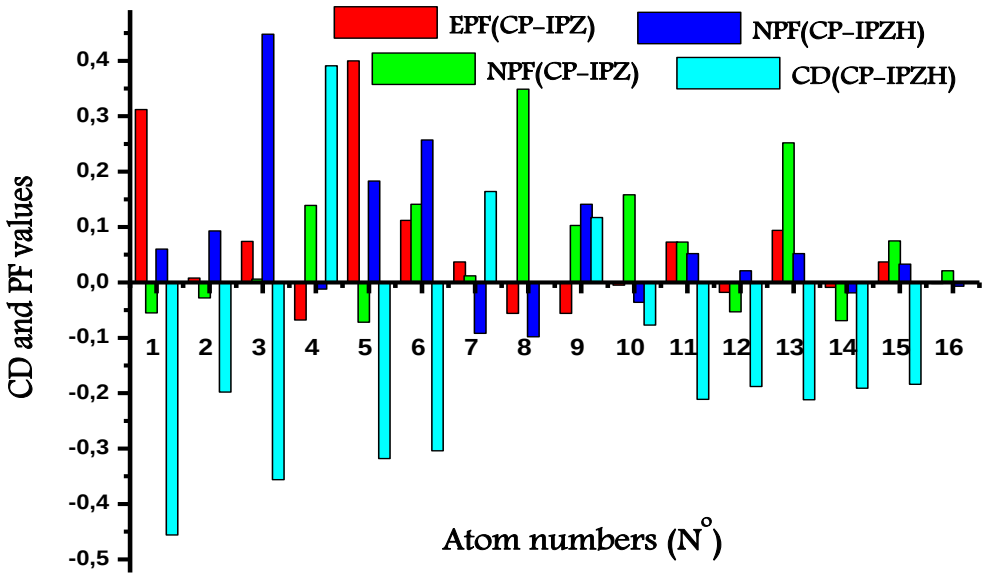

Figure 6. Graphic representation for EPF and NPF values of CP-IPZ and for NPF and CD values of CP-IPZH.

From Table 1 and Figure 6, the N_1 atom of CP-IPZ has a great tendency to be protonated (high NPF value) and the same result was proved according to calculations obtained by MarvinSketch software (cf. §3.1.).

From Figures 1 and 2, the following atoms of CP-IPZH such as N_1, N_2, N_3, C_5, C_6, C_{11}, C_{12}, C_{13}, C_{14} and C_{15} have an ability to interact and/or share their excess electrons with electron-deficient regions of the metal. On the other hand, the atoms, which present a deficit of electrons (C_4, H_{17} and C_7), can bond with the regions of the metal, which have excess electrons. These results indicate that the CP-IPZH inhibitor can adhere to the metal surface through two modes of interaction: *i*) chemical (covalent) and *ii*) physical (non-covalent) which may be due to dipole-dipole interactions, induced dipole-dipole and induced dipole-induced dipole. The presence of one and/or two principle interaction modes will be confirmed in the rest of the work using RDR analysis.

3.2.1.2. NBED analysis using QTAIM theory

In order to contribute more understanding of the local reactivity associated with the nitrogen (N_1, N_2 and N_3) and chlorine (Cl_{12}) atoms of CP-IPZ (non-protonated form) and CP-IPZH (protonated form), non-bonding electron density (NBED), which calculated according to the QTAIM theory are calculated and deliberated (Figures 7 and 8).

Based on the results of the QTAIM analysis (Figures 7 and 8), it can be seen that for the inhibitors studied, the N_1 and N_3 atoms have sufficient NBED values (close to 2e for N_3 in the protonated form CP-IPZH or greater than 2e for N_1 and N_3 in the neutral form CP-IPZ) to be able to form bonds with the electron-deficient regions of the metal. In contrast, the chlorine atom is associated with an insufficient NBED value (well below 6e), which could be due to the delocalisation of the valence electron density of chlorine under the mesomeric +M effect. Furthermore, Figure 8 shows that the NBEDs of CP-IPZ atoms are distinct from those of CP-IPZH atoms, indicating that the NBEDs are highly sensitive to protonation. Given the complexity of the electrochemical interface and inhibition processes, NBEDs may also be sensitive to other factors such as the interaction with the steel surface as well as the nature and concentration of the electroactive species contained in the corrosive solution. Therefore, blind interpretation of NBED results obtained for the inhibitor molecule alone, without taking into account all the relevant factors that may influence their correct determination, may lead to erroneous conclusions.

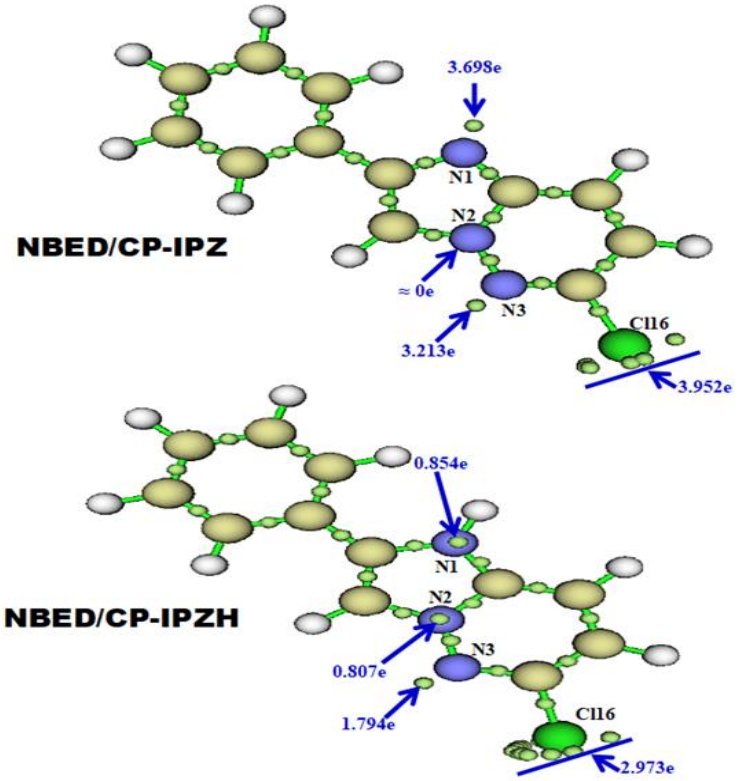

Figure 7. NBED values over the mains atoms of CP-IPZ and CP-IPZH.

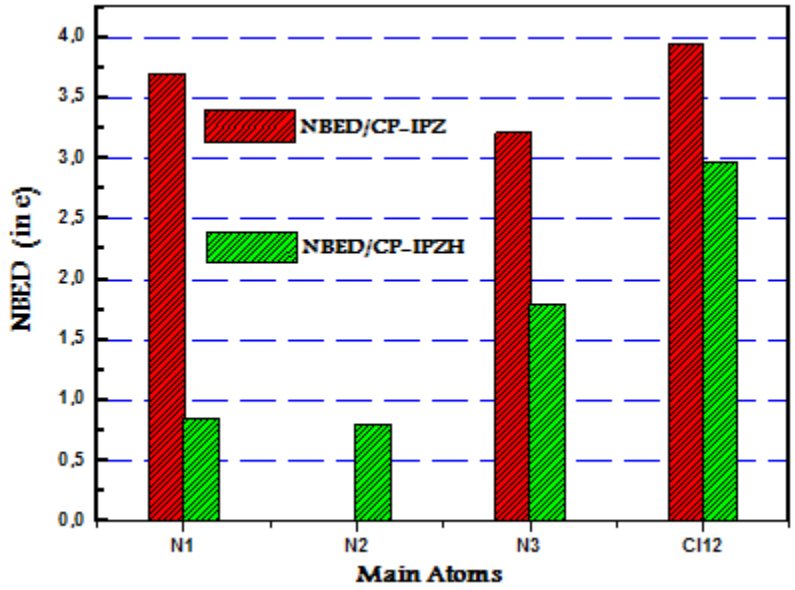

Figure 8. Graphic illustration of NBED over the main atoms of CP-IPZ and CP-IPZH.

Local reactivity indices for activated sites in an isolated inhibitor, although they can provide useful information for anticipating how molecules interact with metal surfaces, should not be considered as true adsorption factors, as is sometimes assumed in the literature, and should therefore be interpreted with caution. In fact, they generally do not take into account the specific interactions at the metal-inhibitor interface, the aggressiveness of the corrosive solution and the solvation effects, which can now play a decisive role in the adsorption of the inhibitor on the steel surface and in the stability of this adsorption. By neglecting these effects, the results obtained may not be representative of the real interactions between the inhibitor and the steel surface in a hydrochloric acid solution. It is therefore essential to take these factors into account in the following sections of this document in order to be able to interpret the results more accurately and to strengthen the correlation between theoretical and experimental results.

3.2.2. GEDT study at TS

In order to take into account the interaction of the inhibitor with the steel surface for a better understanding of the inhibition mechanism, we attempted to study the GEDT property at the transition state (TS) level. To this end, an empirical Grimme GD3 dispersion scheme was added to the B3LYP function of the DFT theory. Unlike the B3LYP function, the corrected B3LYP-GD3 function appears to be reliable for studying GEDT in the transition state [21].

The main purpose of the calculation of the global electron density transfer (GEDT) in the transition states which correspond to the three possibilities of adsorption of CP-IPZH on the steel surface (Figure 9) is to evaluate the quantity of electrons exchanged between the inhibitor and the steel surface.

This approach is suggested by several theorists because it evaluates the GEDT from the donor fragment to the acceptor one at the transition state and not at the state in which the inhibitor and the surface are separated, something that we see more appropriate for better examination of the global electron density transfer for the studied complexes such as Fe@N1-CP-IPZH, Fe@N2-CP-IPZH and Fe@N3-CP-IPZH (Figure 9). Unfortunately, this property is frequently evaluated in the corrosion inhibition topic by the following formula which we see meaningless since it deals with the transfer of electrons in the separate state of inhibitor and bulk iron (Fe(110)) [22–24].

$$\Delta N_{(110)} = \frac{\left(\chi_{Fe(110)} - \chi_{inh}\right)}{2\left(\eta_{Fe(110)} + \eta_{inh}\right)} \quad (3)$$

Therefore, the computed GEDT at the TSs (Figure 9) is increased in the following order: TS(Fe@N3-CP-IPZH)>TS(Fe@N1-CP-IPZH)>TS(Fe@N2-CP-IPZH). Otherwise, the length inhibitor-surface at TS increased as follows TS(Fe@N3-CP-IPZH)<TS(Fe@N1-CP-IPZH)<TS(Fe@N2-CP-IPZH). These results exhibit the following trend of the interaction strength for the studied inhibitor: $N_3>N_1>N_2$. This is in good accordance with the trend obtained according NBO and QTAIM analysis.

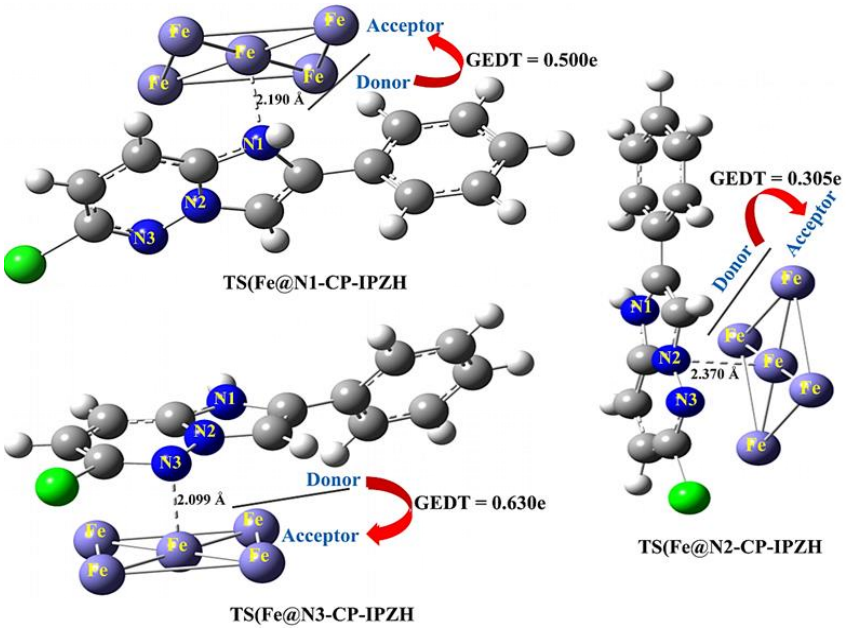

Figure 9. DFT/B3LYP-GD3 calculated of transition states structures for all possible complexes. Distance inhibitor-surface is calculated in Å; GEDT: global electron density transfer.

3.2.3. Kinetic aspect of Fe-complexation

The evaluation of relative free energy (ΔG), activation energy (ΔG_a) and localization of the transition states (TSs) for the proposed complexes (Figure 10) were assessed using QST2

approach. Table 2 shows some theoretical parameters like free energy *G*, relative free energy ΔG and activation energy ΔG_a calculated for all possible complex structures.

Table 2. B3LYP/6-311G^{++}(2d,2p)/LanL2DZ computation for free energy (*G*) and GD3-B3LYP/6-311G^{++}(2d,2p)/LanL2DZ for activation energies (G_a) of TSs leading to the corresponding complexes.

Inhibitor	Stationary points	*G* (a.u)	ΔG_a (kcal·mol^{-1})
CP-IPZH	CP-IPZH+5Fe	–915.2215642	–
	COM1	–964.3702454	–
	COM2	–964.3133529	–
	COM3	–964.3744481	–
	TS-COM1 (B3LYP-GD3)	–915.1394218	51.545
	TS-COM2 (B3LYP-GD3)	–915.1378745	52.516
	TS-COM3 (B3LYP-GD3)	–915.1423254	49.723

Note to Table 2: COM1: Fe@N1-CP-IPZH; COM2: Fe@N2-CP-IPZH; COM3: Fe@N3-CP-IPZH.

According to Table 2, we noticed that the COM3 complex presents the lowest value of ΔG with respect to the other complexes COM1 and COM2. To this result, the thermodynamic stability of the concerned complexes can be abiding by the following trend: COM3>COM1>COM2. This indicates that COM3 has the greatest attachment and non-desorption to the iron surface with respect to COM1 and COM3. In addition, we noticed that the changing of a nitrogen atom (N_1, N_2 then N_3) of the CP-IPZH inhibitor causes an important change in the activation energy barrier, which is higher for N_1 and N_2. This indicates that the coordination of CP-IPZH at N_3 with the iron surface is more kinetically favoured (lower value of ΔG_a) than at N_1 and N_2. This could be attributed probably to the less electron density population around N_1 and N_2 (Figures 8 and 9). These results show that the adsorption of CP-IPZH onto the iron surface is greater in the following order: Fe@N3-CP-IPZH>Fe@N1-CP-IPZH>Fe@N2-CP-IPZH. The same trend was concluded from the computation of GEDT at TS (Figure 9). The energetic barrier (ΔG_a) associated with the three complexation possibilities is illustrated in Figure 10.

Hence, natural atomic charges, calculated according to NBO, are used to evaluate the global electron density transfer GEDT at TS transition states. GEDT represents the sum of the natural atomic charges of the chemical species involved in the reaction, thus quantifying the net electron transfer during the inhibitor-iron interaction. It should be noted that although NBO analysis is widely used to assess natural atomic charges and electron density transfer, it does have certain limitations. These include approximations and simplifications inherent to the method, as well as the dependence of the result on the choice of database and other calculation parameters. It is therefore important to take these limitations into account, and to consider the results obtained by other approaches, in order to obtain a complete understanding of electron density transfer at the transition state level.

Quantum approaches are all based on static calculations and do not take into account the dynamics of corrosion and inhibition reactions. This means that kinetic processes and temporal changes in inhibitor adsorption and corrosion reaction are not taken into account, limiting the ability to fully understand the inhibition mechanism in a dynamic context. In addition, solvent effects are often implicitly incorporated using continuum solvent models or electrostatic potentials. The concentration of the corrosive medium, the properties of substrates (structural defects, composition,) and many others, still remain a challenge to correctly model the corrosion inhibition phenomenon.

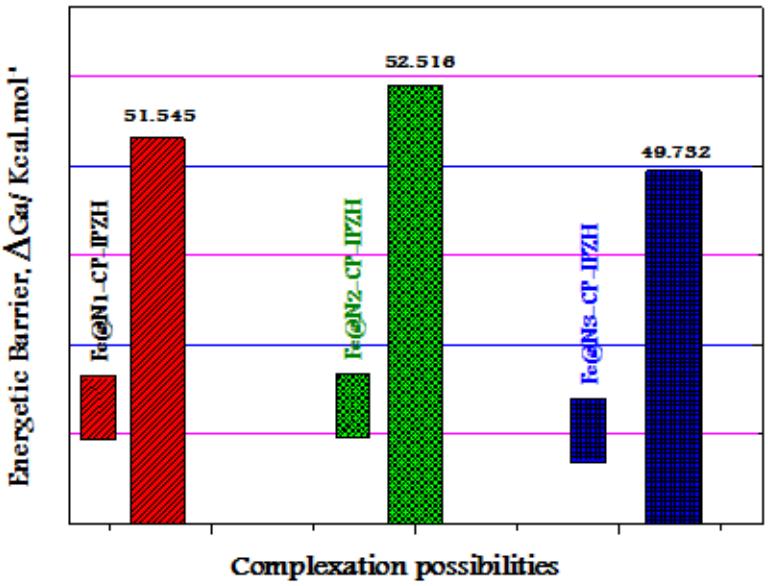

Figure 10. Graphic illustration of the three complexation possibilities.

Despite these limitations, quantum mechanical calculations can still provide valuable information on the electronic properties of inhibitor molecules and contribute to a deeper understanding of the corrosion inhibition mechanism. However, an integrated approach combining quantum mechanical calculations with molecular dynamics simulations, experimental studies and more complete models taking into account the complex interactions in the real system may be necessary for a complete study of the phenomenon.

3.3. MC and MD simulations results

In order to highlight the concentration effect of the corrosive solution and the dynamic aspect of the adsorption process of the inhibitor on the steel surface, MC and MD simulations were carried out to study the adsorption behaviour of the inhibitor examined in its neutral form (CP-IPZ) and in its protonated form (CP-IPZ-H) with an ionic system of $600H_2O+5H_3O^+ + 5Cl^-$ (1 M HCl medium) and $600H_2O+25H_3O^+ + 25Cl^-$ (5 M HCl medium) on the Fe(110) surface. The adsorption configurations and positions of the inhibitor molecules studied in neutral (CP-IPZ) and protonated (CP-IPZH) forms on the Fe(110) substrate are shown in Figures 11 and 12.

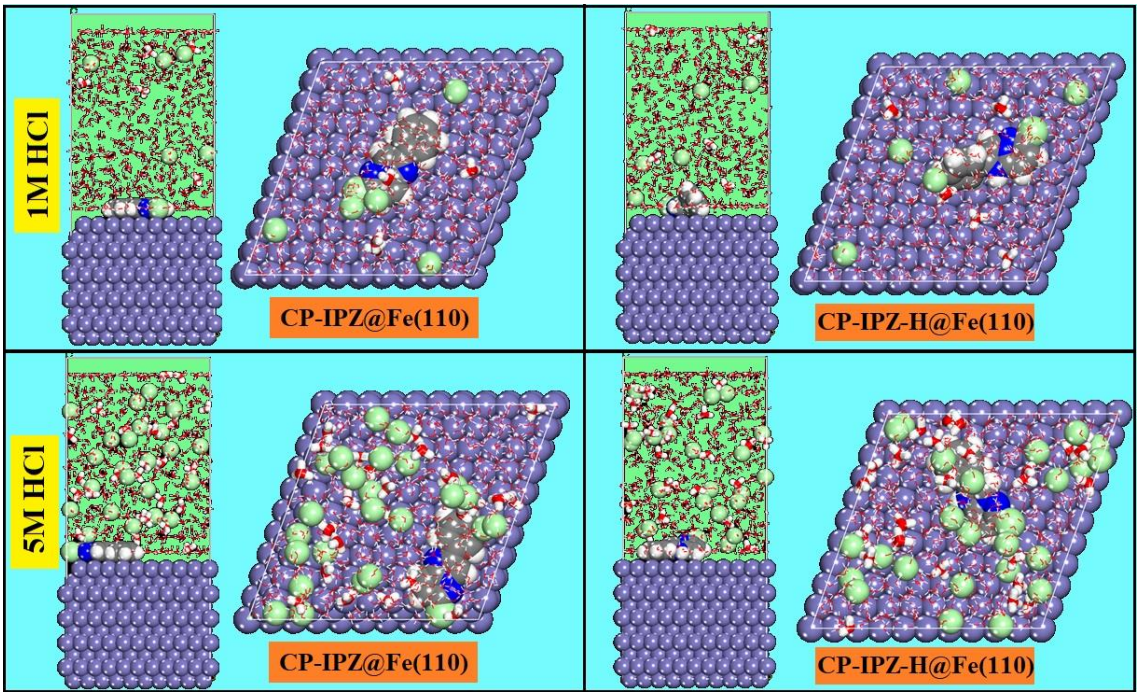

Figure 11. MC simulation results adsorption configurations and positions of the neutral (CP-IPZ) and protonated (CP-IPZ-H) inhibitor forms were adopted with: $600H_2O+5H_3O^+ +5Cl^-$ (1 M HCl medium) and $600H_2O+25H_3O^+ +25Cl^-$ (5 M HCl medium) ions system on Fe(110) surface.

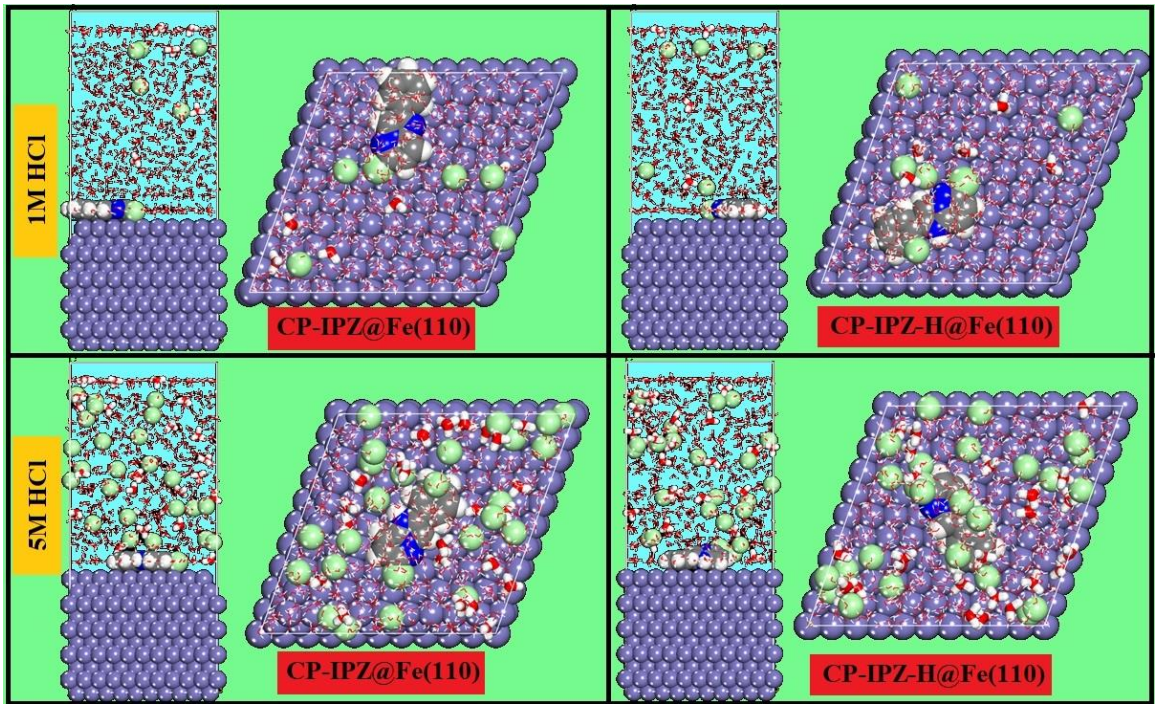

Figure 12. Equilibrium adsorption configuration of CP-IPZ (Neutral) and CP-IPZ-H (Protonated) inhibitor forms were adopted with: $600H_2O+5H_3O^+ +5Cl^-$ (1 M HCl medium) and $600H_2O+25H_3O^+ +25Cl^-$ (5 M HCl medium) ions system on Fe(110) surface, obtained *via* MD.

The adsorption energies (E_{ads}) are calculated and then represented in Figure 13. For the distribution of the E_{ads} for the neutral (CP-IPZ) and protonated (CP-IPZ-H) onto the Fe(110) substrate in the both media by MC simulations.

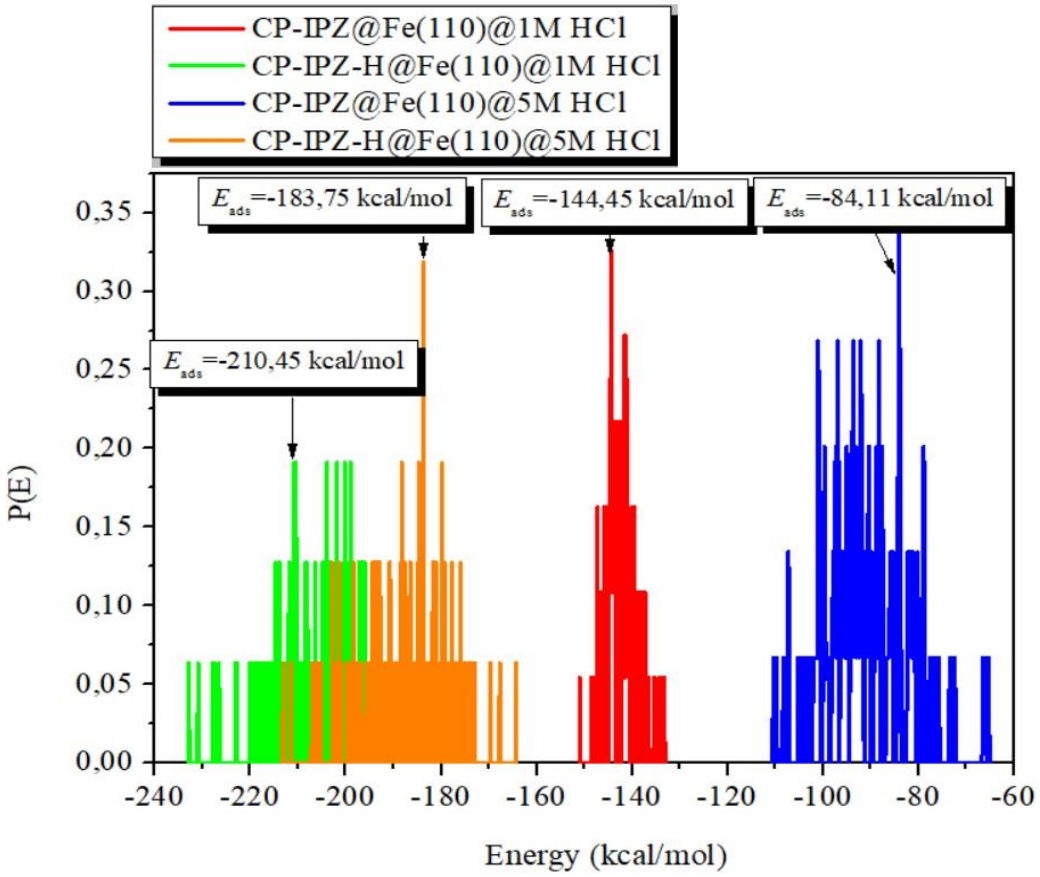

Figure 13. Adsorption energy distribution curves for neutral (CP-IPZ) and protonated (CP-IPZ-H) inhibitor forms were adopted with: $600H_2O+5H_3O^+ + 5Cl^-$ (1 M HCl medium) and $600H_2O+25H_3O^+ + 25Cl^-$ (5 M HCl medium) ions system on Fe(110) surface, obtained *via* MC.

According these results, the values of E_{ads} can be classified according to the following order: protonated CP-IPZ-H in 1 M HCl medium (-210.75 kcal·mol^{-1})>protonated CP-IPZ-H in 5 M HCl medium (-183.75 kcal·mol^{-1})>neutral CP-IPZ in 1 M HCl medium (-144.45 kcal·mol^{-1})>neutral CP-IPZ in 5 M HCl medium (-84.11 kcal·mol^{-1}). Based on the obtained values, tested inhibitor shows a remarkable affinity toward Fe(110) surface. This leads to the formation of a layer on the metal surface that prevents the passage of corrosive agents into protected surface [25, 26]. On the other hand, it can be noted that the CP-IPZ-H form in both media demonstrates more tendency to adsorb on the metal surface in comparison with CP-IPZ form in the both media. Consequently, protonated inhibitor in both media can form more strongly adherent protective film upon metal surface and then can offer better protection character against corrosion than neutral form. Similar trend has been reported in the literature [27]. Besides, it is clear from Figures 12 and 13 that the inhibitor

molecules are placed closely to the surface, which underlined their ability to interact with the surface. Furthermore, the adsorption geometry of both forms of inhibitor on the Fe(110) surface in both media exhibits a parallel orientation, involving almost its entire molecular skeleton. In this context, it is well recognized that parallel adsorption configuration of an inhibitor can provide an enhanced metal coverage, consequently good protection against corrosion [28, 29]. These results confirm the trend in experimental inhibitory efficiencies recorded in the presence of a 10^{-3} M concentration of CP-IPZ in 1 M and 5 M hydrochloric acid solutions, but they are still insufficient to justify the large difference in polarisation resistance observed in both media.

3.3.1. Radial distribution function (RDF)

To complement the geometric investigation of the adsorption behaviors of studies inhibitor, the radial distribution function (RDF) was analyzed. RDF is a suitable computational tool to estimate the length of bond between the adsorbed inhibitor molecule and the target surface. It is well known that the inter-atomic distance between 1.0 and 3.5 Å is generally associated with the chemical bonding, whereas non-bonding one (*i.e.* physical interaction) corresponding to distance longer than 3.5 Å [30, 31].

In our case, Figure 14 summarizes the distance between iron atoms and N and Cl atoms of inhibitor in its both forms and for the both media, which correspond to the highest peak of RDF curves. As can be seen from Figure 14, except Fe–N_3 (3.31 Å) for CP-IPZ, Fe–N_3 (3.17 Å) for CP-IPZ-H in 1 M HCl medium, Fe–N_3 (3.13 Å) for the both forms (CP-IPZ and CP-IPZ-H) in 5 M HCl medium, all the inter-atomic distances are less than 3.5 Å, which indicates that chemical bonding can be manifested between the tested inhibitor molecule and protected surface in its both forms and for the both media.

It is interesting to note that the difference in adsorption energy of the CP-IPZH (majority form) evaluated in the corrosive media 1 M and 5 M HCl hardly exceeds 27 $kcal \cdot mol^{-1}$, whereas the experimental study clearly shows that the difference in terms of steel resistance in the two environments considered is now quite substantial, of the order of almost 900 $\Omega \cdot cm^2$. It should also be noted that the orders of magnitude of the Fe–N and Fe–Cl bonds are practically very comparable and less than 3.31 Å, which argues in favour of chemisorption, whatever the aggressiveness of the medium, and moreover for both forms of the inhibitor molecule, protonated or not. In this respect, Kokalj [1] stressed that molecular parameters are only indicators, and that indicators are most useful when they show clear trends with significant differences. He also stated that Equation (1) commonly used in the literature to calculate adsorption energies is adequate for structural relaxations, whereas its usefulness for MD is questionable. This means that small differences should not be relied upon, even if the parameters have been carefully obtained through rigorous and convergent calculations carried out according to highly advanced theoretical principles and taking into account the various factors contributing to the complexity of the system under study.

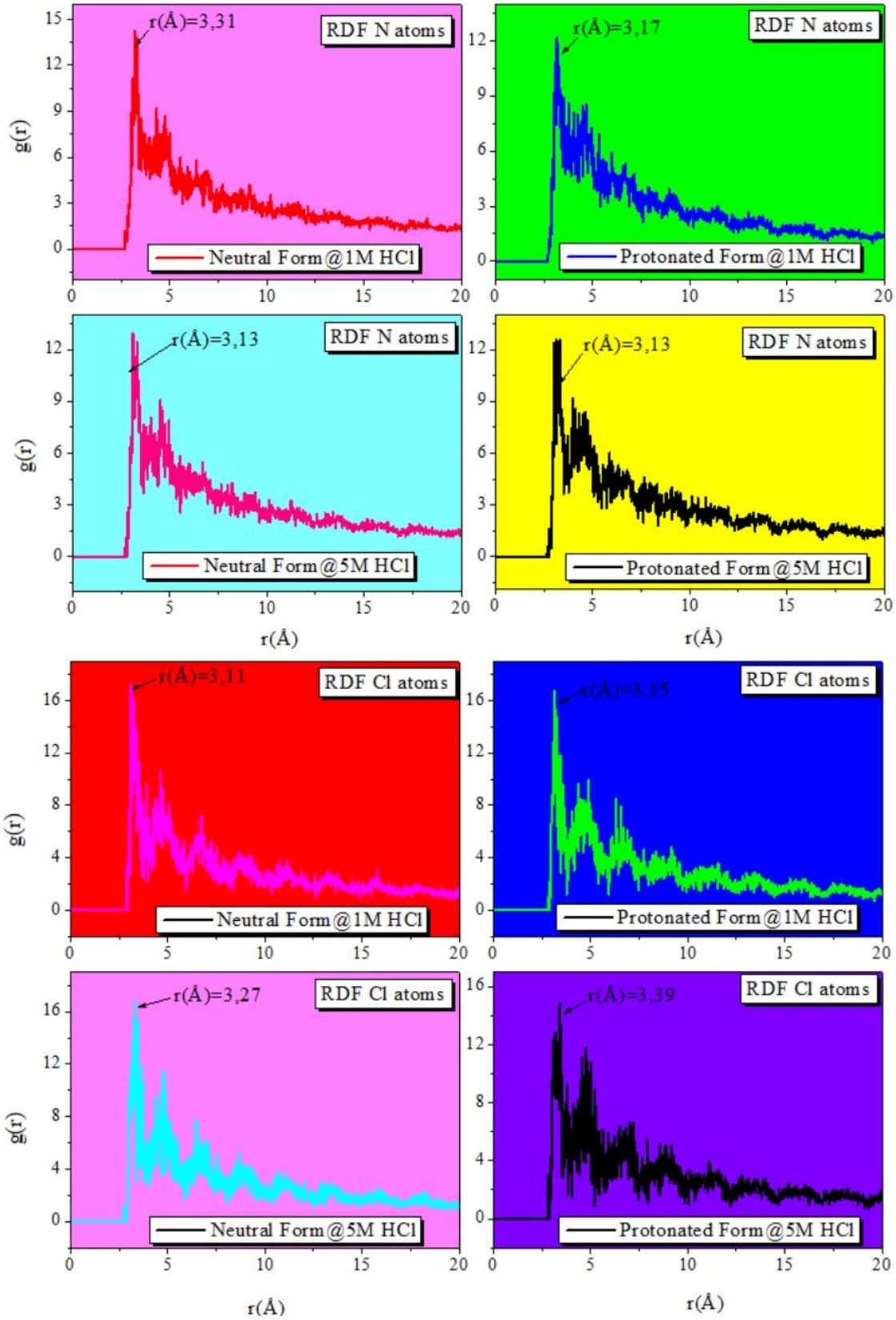

Figure 14. RDF of the N and Cl atoms of the neutral and protonated forms were adopted with: $600H_2O+5H_3O^+ +5Cl^-$ (1 M HCl medium) and $600H_2O+25H_3O^+ +25Cl^-$ (5 M HCl medium) ions system on Fe(110) surface, obtained *via* MD.

In addition, all the tests in the dynamic simulations are carried out on a reticular plane (110) of the iron. Assuming that the steel can be assimilated to pure iron with a centered cubic structure, it is therefore essential to interpret the results obtained by the MD simulations with great caution, particularly when it comes to correlating them with the (experimental) corrosion resistance of real steel in an aggressive solution containing an inhibitor. This is because the corrosion resistance of the steel depends not only on the concentration and composition of the aggressive solution and the structure of the inhibitor, but also on many factors such as its heterogeneous chemical composition, its structural characteristics (crystalline structure, roughness, and calamine defect).

All these considerations once again justify the fact that, despite all our efforts to approximate the real electrochemical system, the theoretical calculation still falls short of our expectations.

4. Conclusion

- The microspecies distribution diagram of the CP-IPZ molecule, obtained from the distribution of partial atomic charges calculated using Marvinsketch software, shows that the neutral form CP-IPZ is very unstable at pH < ($pK_a - 2 = 0.3$) and transforms entirely into CP-IPZH (protonated form), thus becoming an ultra-majority form with a percentage of almost 100% in the electrolytic solution. In addition, the N_3 nitrogen atom in CP-IPZH has the highest charge density, which may give it the ability to coordinate with the iron atoms that make up C38 steel.
- The local reactivity indices (NPF) calculated according to (NBO) and not according to (NPA) as well as the charge distribution of the CP-IPZH atoms, showed that the nitrogen atoms (N_1, N_2, N_3) present the greatest capacity to interact and/or to share their excess electrons with the regions of the metal, which present a deficit in electrons.
- The results of the QTAIM analysis indicate that, for the two forms of inhibitor studied, the N_1 and N_3 atoms have sufficient NBED values (close to 2e for N_3 in the protonated form CP-IPZH and greater than 2e for N_1 and N_3 in the neutral form CP-IPZ), which could allow them to form bonds with the electron-deficient regions of the metal.
- The CD, EPF, NPF and NEBD values for the protonated and non-protonated forms of the isolated molecule (CP-IPZ) are distinct, indicating that they are overly sensitive to protonation, and therefore to the molecular geometry used as a starting point in the calculations. It is important to note that the above parameters can also vary depending on the interactions of the inhibitor molecules with the steel surface, and the nature and concentration of the electro-active species contained in the corrosive solution.
- The results of the GEDT global electron density transfer, evaluated at the transition state (TS) level in order to take into account the metal-inhibitor interaction, and those of the free energies ΔG as well as the activation energies ΔG_a showed that the adsorption of CP-IPZH on the iron surface occurs more prominently in the following order: Fe@N_3-CP-IPZH>Fe@N_1-CP-IPZH>Fe@N_2-CP-IPZH confirming previous results.

All the theoretical approaches mentioned above provide only limited information on interactions between the inhibitor and the metal surface in the static state and do not take into account the effects of the aggressiveness of the corrosive medium. Consequently, they cannot be useful to predict the difference in inhibition behaviour of CP-IPZ in 1 M and 5 M HCl. In fact, ignoring these factors can lead to unrepresentative results or significant biases.

The results of the MD and MC studies, which aim to take into account the inhibitor-metal interactions, the effect of the nature and concentration of the electro-active species present in the corrosive solution and the dynamic aspect of the inhibitor adsorption process on the steel surface, show that the protonated form CP-IPZH exhibits interesting inhibiting properties compared to the neutral form CP-IPZ in 1 M and 5 M HCl due to the difference in their adsorption energies. In addition, both forms of inhibitor adsorb onto the Fe(110) surface in both media by adopting a parallel orientation at a distance of less than 3.5 Å, which is often interpreted in the literature as if the inhibitor involved almost its entire molecular skeleton, thus blocking the oxidation reaction at more active sites on the steel surface *via* chemical adsorption.

On the other hand, the small difference recorded between the adsorption energy of CP-IPZH (ultra-majority form) in 1 M and 5 M HCl, combined with the large difference in experimental polarization resistance recorded in these two media in the presence of the same inhibitor concentration, constitute serious reasons for questioning previous interpretations. It is important to not attribute protective performance solely to adsorption, but rather to consider it as one of the factors controlling protection. In the same vein, we note that Kokalj in reference [1] stated that it is essential to recognize that molecular parameters are only indicators and that indicators are most useful when they show clear trends with significant differences. It is therefore necessary not to rely on small differences in order to avoid ambiguous interpretations. It is also important to bear in mind that molecular dynamics results must be interpreted with caution when transferred to real conditions. Experimental conditions may differ from simulation conditions for reasons of feasibility (for example, the (110) iron plane is often chosen to avoid the complexity of modeling steel characteristics), which may lead to discrepancies between molecular dynamics and experimental results. All these considerations once again justify the fact that, despite all our efforts to approximate the real electrochemical system, the theoretical calculation still falls short of our expectations.

To make progress in understanding the mechanical aspects of corrosion inhibition, the corresponding modeling must take more and more factors into account, as there are huge gaps to be filled, involving several orders of magnitude of length and time scales. With this in mind, multi-scale modeling using the ICME paradigm should be the new way forward.

Acknowledgements

The authors also extend their appreciation to the Moroccan Association of Theoretical Chemists (AMCT) for access to the computational facility.

References

1. A. Kokalj, Molecular modeling of organic corrosion inhibitors: calculations, pitfalls, and conceptualization of molecule–surface bonding, *Corros. Sci*., 2021, **193**, 109650. doi: 10.1016/j.corsci.2021.109650
2. G. Gece, The use of quantum chemical methods in corrosion inhibitor studies, *Corros. Sci*., 2008, **50**, no. 11, 2981–2992. doi: 10.1016/j.corsci.2008.08.043
3. A. Kokalj, Is the analysis of molecular electronic structure of corrosion inhibitors sufficient to predict the trend of their inhibition performance, *Electrochim. Acta*, 2010, **56**, no. 2, 745–755. doi: 10.1016/j.electacta.2010.09.065
4. A. Kokalj, M. Lozinsek, B. Kapun, P. Taheri, S. Neupane, P. Losada-Peez, C. Xie, S. Stavber, D. Crespo, F.U. Renner, A. Mol and I. Milosev, Simplistic correlations between molecular electronic properties and inhibition efficiencies: do they really exist? *Corros. Sci*., 2021, **179**, 108856. doi: 10.1016/j.corsci.2020.108856
5. A. Kokalj, On the alleged importance of the molecular electron-donating ability and the HOMO–LUMO gap in corrosion inhibition studies, *Corros. Sci*., 2021, **180**, 109016. doi: 10.1016/j.corsci.2020.109016
6. H. El Assiri, M. Driouch, Z. Bensouda, M. Beniken, A. Elhaloui, M. Sfaira and T. Saffaj, Computational study and QSPR approach on the relationship between corrosion inhibition efficiency and molecular electronic properties of some benzodiazepine derivatives on C-steel surface, *Anal. Bioanal. Chem*., 2019, **11**, no. 3, 373–395.
7. A. Kokalj, On the HSAB based estimate of charge transfer between adsorbates and metal surfaces, *Chem. Phys*., 2012, **393**, no. 1, 1–12. doi: 10.1016/j.chemphys.2011.10.021
8. N. Kovačević, I. Milošev and A. Kokalj, The roles of mercapto, benzene, and methyl groups in the corrosion inhibition of imidazoles on copper: Ⅱ. Inhibitor–copper bonding, *Corros. Sci*., 2015, **98**, 457–470. doi: 10.1016/j.corsci.2015.05.041
9. P. Morales-Gil, M. Walczak, R. Cottis, J. Romero and R. Lindsay, Corrosion inhibitor binding in an acidic medium: interaction of 2-mercaptobenizmidazole with carbon-steel in hydrochloric acid, *Corros. Sci*., 2014, **85**, 109–114. doi: 10.1016/j.corsci.2014.04.003
10. El H. El Assiri, M. Driouch, Z. Bensouda, F. Jhilal, T. Saffaj, M. Sfaira and Y. Abboud, Quantum chemical and QSPR studies of bis-benzimidazole derivatives as corrosion inhibitors by using electronic and lipophilic descriptors, *Desalin. Water Treat*., 2018, **111**, 208–225. doi: 10.5004/dwt.2018.22198
11. Z. Lakbaibi, M. Damej, A. Molhi, M. Benmessaoud, S. Tighadouini, A. Jaafar, T. Benabbouha, A. Ansari, A. Driouich and M. Tabyaoui, Evaluation of inhibitive corrosion potential of symmetrical hydrazine derivatives containing nitrophenyl moiety in 1 M HCl for C38 steel: experimental and theoretical studies, *Heliyon*, 2022, **8**, E09087. doi: 10.1016/j.heliyon.2022.e09087

12. Z. Lakbaibi, A. Jaafar, A.E. Aatiaoui and M. Tabyaoui, Effect of the explicit solvation of 2-propanol on the Darzens reaction mechanism: a computational study, *Comput. Theor. Chem*., 2022, **1209**, 113628.
13. O. Dagdag, Z. Safi, H. Erramli, N. Wazzan, I. Obot, E. Akpan, C. Verma, E.E. Ebenso, O. Hamed and A. El Harfi, Anticorrosive property of heterocyclic based epoxy resins on carbon steel corrosion in acidic medium: electrochemical, surface morphology, DFT and Monte Carlo simulation studies, *J. Mol. Liq*., 2019, **287**, 110977. doi: 10.1016/j.molliq.2019.110977
14. E. Berdimurodov, A. Kholikov, K. Akbarov, L. Guo, S. Kaya, K.P. Katin, D.K. Verma, M. Rbaa, O. Dagdag and R. Haldhar, Novel gossypol–indole modification as a green corrosion inhibitor for low–carbon steel in aggressive alkaline–saline solution, *Colloids Surf., A*, 2022, **637**, 128207. doi: 10.1016/j.colsurfa.2021.128207
15. R. Haldhar, D. Prasad, I. Bahadur, O. Dagdag, S. Kaya, D.K. Verma and S.C. Kim, Investigation of plant waste as a renewable biomass source to develop efficient, economical and eco-friendly corrosion inhibitor, *J. Mol. Liq*., 2021, **335**, 116184. doi: 10.1016/j.molliq.2021.116184
16. I.B. Obot, K. Haruna and T.A. Saleh, Atomistic simulation: a unique and powerful computational tool for corrosion inhibition research, *Arabian J. Sci. Eng*., 2019, **44**, 1–32. doi: 10.1007/s13369-018-3605-4
17. D.S. Chauhan, M.A. Quraishi, A.A. Sorour, S.K. Saha and P. Banerjee, Triazole-modified chitosan: a biomacromolecule as a new environmentally benign corrosion inhibitor for carbon steel in a hydrochloric acid solution, *RSC Adv*., 2019, **9**, 14990–15003. doi: 10.1039/c9ra00986h
18. A. Dutta, S.K. Saha, U. Adhikari, P. Banerjee and D. Sukul, Effect of substitution on corrosion inhibition properties of 2-(substituted phenyl) benzimidazole derivatives on mild steel in 1 M HCl solution: a combined experimental and theoretical approach, *Corros. Sci*., 2017, **123**, 256–266. doi: 10.1016/j.corsci.2017.04.017
19. W. Daoudi, A. El Aatiaoui, N. Falil, M. Azzouzi, A. Berisha, L.O. Olasunkanmi, O. Dagdag, E.E. Ebenso, M. Koudad, A. Aouinti, M. Loutou and A. Oussaid, Essential oil of *Dysphania Ambrosioides* as a green corrosion inhibitor for mild steel in HCl solution, *J. Mol. Liq*., 2022, **363**, 119839. doi: 10.1016/j.molliq.2022.119839
20. R. Ganjoo, S. Sharma, A. Thakur, H. Assad, P.K. Sharma, O. Dagdag, A. Berisha, M. Seydou, E.E. Ebenso and A. Kumar, Experimental and theoretical study of sodium cocoyl glycinate as corrosion inhibitor for mild steel in hydrochloric acid medium, *J. Mol. Liq*., 2022, **364**, 119988. doi: 10.1016/j.molliq.2022.119988
21. X.Y. Zhang, Q.X. Kang and Y. Wang, Theoretical study of *N*-thiazolyl-2-cyanoacetamide derivatives as corrosion inhibitor for aluminum in alkaline environments, *Comput. Theor. Chem*., 2018, **1131**, 25–32. doi: 10.1016/j.comptc.2018.03.026
22. L. Guo, S. Zhu and S. Zhang, Experimental and theoretical studies of benzalkonium chloride as an inhibitor for carbon steel corrosion in sulfuric acid, *J. Ind. Eng. Chem*., 2015, **24**, 174–180. doi: 10.1016/j.jiec.2014.09.026

23. A. Singh, K. Ansari, M. Quraishi, S. Kaya and L. Guo, Aminoantipyrine derivatives as a novel eco-friendly corrosion inhibitors for P110 steel in simulating acidizing environment: experimental and computational studies, *J. Nat. Gas Sci. Eng*., 2020, **83**, 103547. doi: 10.1016/j.jngse.2020.103547
24. F. Benhiba, H. Serrar, R. Hsissou, A. Guenbour, A. Bellaouchou, M. Tabyaoui, S. Boukhris, H. Oudda, I. Warad and A. Zarrouk, Tetrahydropyrimido-triazepine derivatives as anti-corrosion additives for acid corrosion: chemical, electrochemical, surface and theoretical studies, *Chem. Phys. Lett*., 2020, **743**, 137181. doi: 10.1016/j.cplett.2020.137181
25. R. Oukhrib, B. El Ibrahimi, H.A. Oualid, Y. Abdellaoui, S. El Issami, L. Bazzi, M. Hilali and H. Bourzi, In silico investigations of alginate biopolymer on the Fe(110), Cu(111), Al(111) and Sn(001) surfaces in acidic media: quantum chemical and molecular mechanic calculations, *J. Mol. Liq*., 2020, **312**, 113479. doi: 10.1016/j.molliq.2020.113479
26. B. El Ibrahimi, L. Bazzi and S. El Issam, The role of PH in corrosion inhibition of tin using the proline amino acid: theoretical and experimental investigations, *RSC Adv*., 2020, **10**, no. 50, 29696. doi: 10.1039/D0RA04333H
27. K. Chkirate, K. Azgaou, H. Elmsellem, B. El Ibrahimi, N.K. Sebbar, E.H. Anouar, M. Benmessaoud, S. El Hajjaji and El M. Essassi, Corrosion inhibition potential of 2-[(5-methylpyrazol-3-yl)methyl]benzimidazole against carbon steel corrosion in 1 M HCl solution: combining experimental and theoretical studies, *J. Mol. Liq*., 2021, **321**, 114750. doi: 10.1016/j.molliq.2020.114750
28. H. Bourzi, R. Oukhrib, B. El Ibrahimi, H.A. Oualid, Y. Abdellaoui, B. Balkard, M. Hilali and S. El Issami, Understanding of anti-corrosive behavior of some tetrazole derivatives in acidic medium: adsorption on Cu(111) surface using quantum chemical calculations and *Monte Carlo* simulations, *Surf. Sci*., 2020, **702**, 121692. doi: 10.1016/j.susc.2020.121692
29. B. El Ibrahimi, A. Jmiai, K. El Mouaden, A. Baddouh, S. El Issami, L. Bazzi and M. Hilali, Effect of solution's pH and molecular structure of three linear α-amino acids on the corrosion of tin in salt solution: a combined experimental and theoretical approach, *J. Mol. Struct*., 2019, **1196**, 105–118. doi: 10.1016/j.molstruc.2019.06.072
30. V. Srivastava, J. Haque, C. Verma, P. Singh, H. Lgaz, R. Salghi and M.A. Quraishi, Amino acid based imidazolium zwitterions as novel and green corrosion inhibitors formild steel: experimental, DFT and MD studies, *J. Mol. Struct*., 2017, **244**, 340–352. doi: 10.1016/j.molliq.2017.08.049
31. A. Singh, K.R. Ansari, Y. Lin, M.A. Quraishi, H. Lgaz and I.M. Chung, Corrosion inhibition performance of imidazolidine derivatives for j55 pipeline steel in acidic oilfield formation water: electrochemical, surface and theoretical studies, *J. Taiwan Inst. Chem. Eng*., 2019, **95**, 341–356. doi: 10.1016/j.jtice.2018.07.030

♦ ♦ ♦